

# **Sub-pixel Evaluation with Frequency Response Analysis**

Koji OKAMOTO

Nuclear Engineering Research Laboratory,  
The University of Tokyo,  
Tokai-mura, Ibaraki, 319-1188, Japan  
*okamoto@utnl.jp*

**Abstract:** The frequency responses on the sub-pixel evaluation technique were investigated using the Monte-calro Simulation technique. The frequency response by the FFT based cross-correlation gives very good results, however, the gain loss does exist for the small displacement, (less than 0.5 pixel). While, the no gain loss is observed in the Direct Cross-correlation, however, the sub-pixel accuracy was limited to be about 0.1 pixel, i.e., it could not detect the small displacement. To detect the higher accurate sub-pixel displacement, the gradient based technique is the best. For the small interrogation area (e.g., 4x4), only the gradient technique can detect the small displacement correctly.

**Keywords:** PIV, Sub-pixel estimation, Cross-correlation, FFT, Gradient method

## **1. Introduction**

The Particle Image Velocimetry (PIV) is widely used to detect the quantitative characteristics of the fluid flow. Currently, the turbulence structures are analyzed using the PIV results. The dynamic range of the PIV depends on the allowable maximum displacement of the particle and the detectable minimum displacement, sub-pixel.

The error of the PIV evaluation is mainly classified into the erroneous vector and sub-pixel estimation. The erroneous vector is caused by the miss-tracking of the particle (pattern) movement. The error of the erroneous vector is usually bigger than 1 pixel. Lots of error correction techniques, including iterative PIV (Raffel et al., 1999) and correlation multiplication(Hart, 2000), were proposed. The erroneous vectors may be removed easily, when the number of the vector is large enough. While, the sub-pixel error highly relates to the image condition. The amount of the information in the interrogation area determines the sub-pixel accuracy.

In this study, the sub-pixel estimation on the error is focused. The sub-pixel accuracy was also discussed by many researchers(Keane and Adrian, (1990), Westerveel et al., (1997), Raffel et al., (1999)). They evaluated the peak locking, effects of out-of-plane and so on. To improve the sub-pixel accuracy, many techniques were proposed, including three-point Gaussian method. The image distortion techniques were also proposed (Lourendier et al., 1999). In the previous studies, the error on the PIV analysis was focused. The root mean square of the error is usually used for the index of the sub-pixel error. The RMS value is something like the summation of the error. For the turbulence analysis, the frequency responses of the PIV results are also very important. Although the RMS is small, the frequency responses may be bad in certain cases. In this study, the frequency responses on the sub-pixel evaluation technique were investigated using the Monte-calro Simulation technique.

## **2. Evaluation Procedure**

### *2.1 PIV techniques*

In this study, three PIV techniques are evaluated, i.e., the well-known FFT based cross-correlation technique (Raffel et al. 1999), the direct cross-correlation (Raffel et al., 1999), and gradient based technique(Sugii et al.,2000). In FFT, no offset was considered. Using the fixed size interrogation area, the covariant of the two

interrogations was calculated without any offset. In Direct Cross-Correlation (DCC), the correlation coefficient was directly calculated with considering the offset. The difference between FFT and DCC is the consideration of the offset. For the sub-pixel evaluation for the both two correlation techniques, the three-point Gaussian fitting (Raffel et al., 1999) was applied. When the maximum cross-correlation value  $C$  was obtained at  $(i, j)$ ,

$$u = i - \frac{\ln C(i+1, j) - \ln C(i-1, j)}{2(\ln C(i+1, j) - 2 \ln C(i, j) + \ln C(i-1, j))}, \quad (1)$$

For the gradient technique, the iterative procedure was applied to detect the pixel-unit displacement. Then the sub-pixel displacement was detected using the gradient technique (Sugii et al. 2000).

$$u = \frac{\partial g / \partial t}{\partial g / \partial x}, \quad (2)$$

where  $g$  is the intensity of the target point.

To evaluate the frequency response on the PIV results, the synthetic images were generated according to the assumed velocity,  $I$ . Then, using the image, the velocity,  $O$ , was reconstructed by a PIV evaluation algorithm to obtain the transfer function  $I/O$ . Figure 1 schematically shows the  $I/O$  responses. The following velocity distributions were taken as the input velocity,  $I$ .

$$u = A \sin(2\pi f x + \phi). \quad (3)$$

With varying the amplitude  $A$  and the spatial frequency,  $f$ , the output responses were evaluated. In this study, the velocity  $u$  and the frequency  $f$  were determined in the unit of pixel/interval and  $\text{pixel}^{-1}$ , respectively. In this study, the  $x$ -axis image size was set to be 1024 pixel. So, the spatial frequency  $f$  was determined as,  $f = k / 1024$ , where  $k$  is the number of waves in 1024 pixel.

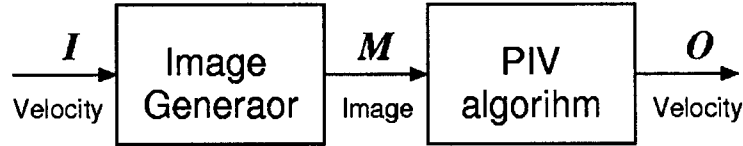


Fig. 1 Concept of the frequency response analysis

## 2.2 Image Generator

As the image generator, the Gaussian particle image with random generator was used (Okamoto et al. 2000). The parameters were, average particle size, standard deviation of particle size, laser light intensity distribution, and number of particles. To clearly obtain the characteristics, no out-of-plane motion was considered without any noise. The fill factor of the CCD was assumed to be 100%.

As the laser light intensity, the Gaussian distribution was applied in  $z$  direction. For the standard case, the particle size was fixed to be 2.0 pixel with standard deviation of 0.5 pixel. This means, the 80% of particle sizes are in the range of 1.5 to 2.5 pixel. Average number of particles is fixed to be 0.06/pixel, ( $N_i \approx 60$  in  $32 \times 32$  interrogation area). The interrogation area was also fixed to be  $32 \times 32$  for standard. Number of the particle was about 60, which is large enough for the sub-pixel analysis for cross-correlation technique.

For the comparison, very small interrogation area was also checked, i.e.,  $4 \times 4$ . The number of particles in  $4 \times 4$  was about 1, which was too small to detect the correct sub-pixel. Example of the generated image is shown in Fig.2, with the interrogation area size.

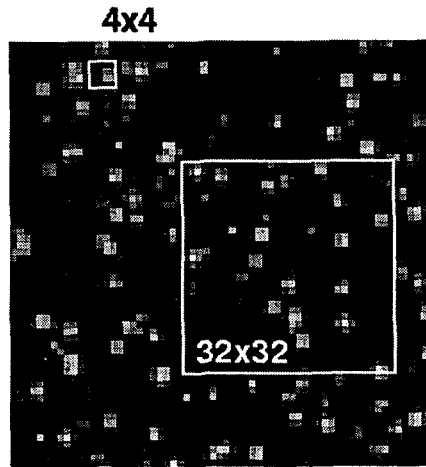


Fig. 2 Example of the generated images

With applying the displacement in Equation (3) to the individual particles, the second image was generated. Using the 1st and 2nd images, the displacement was reconstructed. The parameters of the transfer function were spatial frequency  $f$  and displacement amplitude  $A$ . The spatial frequency  $f$  was varied from 0.001 to 0.06  $\text{pixel}^{-1}$ , i.e., 1 to 64 waves in 1024 pixel. To focus on the sub-pixel evaluation, the amplitude  $A$  was varied from 0.01 to 5 pixel. To reduce the edge effects, fixed phase delay ( $\phi=0.2$ ) was applied in Equation (3).

### 3. Results and discussion

#### 3.1 Velocity distributions

Figure 3 shows the example of the reconstructed velocity (displacement) for the lower frequency ( $f=0.002 \text{ pixel}^{-1}$ ) and smaller amplitude ( $A=0.03 \text{ pixel}$ ). The interrogation area was 32x32. Since there were no noises, the FFT could reconstruct such small amplitude fluctuation. However, the DCC had relatively larger error. The gradient method could reconstruct the sub-pixel displacement much better than that of correlation technique (FFT/DCC).

In the small displacement case, although the cross-correlation factor at  $x=0$  was almost 1.0, the value of the neighbor ( $x = -1$  and 1) contains lots of noise for DCC, resulting in the error for the sub-pixel evaluation.

The cross-correlation function in the FFT could be expressed as the delta function  $\delta(u)$ , analytically. Since

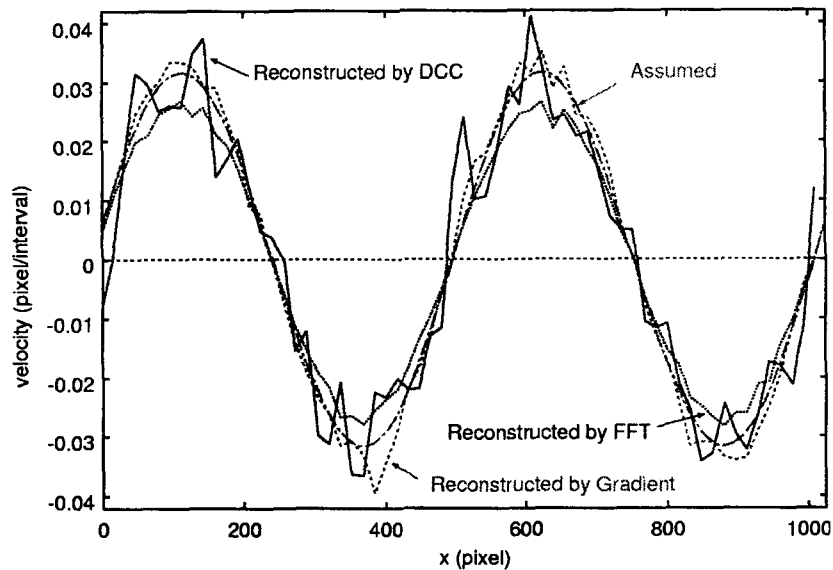


Fig.3 Example of the reconstructed velocity distributions

there were no noises on the image, the FFT could correctly reconstruct the delta function, i.e., narrow Gaussian function.

The reconstructed displacement was then estimated using the least square technique. Since the frequency was already known, the response amplitude and phase delay were calculated. Then the gain could be determined by the ratio of reconstructed amplitude to given amplitude.

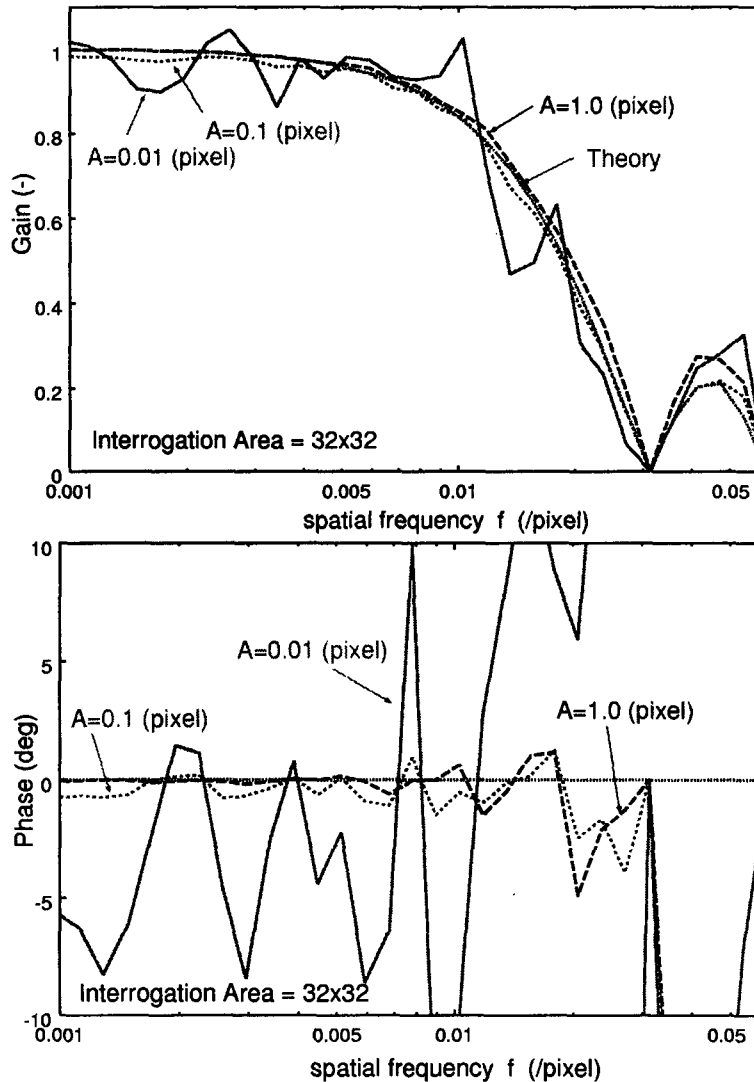
### 3.2 Bode diagram

The Bode diagrams (Gain response and phase delay) for the three techniques are shown in Figures 4 and 5. The red line denotes the theoretical response curve.

$$G = \frac{|\sin(\pi f I)|}{\pi f I} \quad (4)$$

where  $I$  is the interrogation area size, i.e.,  $I=32$  and  $4$  for Figs. 4 and 5, respectively.

In Figure 4, the interrogation area size is  $32 \times 32$ , i.e., number of particles in the area ( $N_I$ ) is about 60. For the DCC, the gain almost followed the theoretical one under the larger amplitude ( $A > 0.1$  pixel). However, in smaller amplitude case ( $A = 0.01$  pixel), it fluctuated because of the larger error. The phase information also supports that the above results. The phase of larger amplitude was in the range of  $\pm 2$  degree. The DCC can reconstruct the



(a) Direct cross-correlation [DCC]

Fig. 4 Bode diagram for  $32 \times 32$  interrogation area

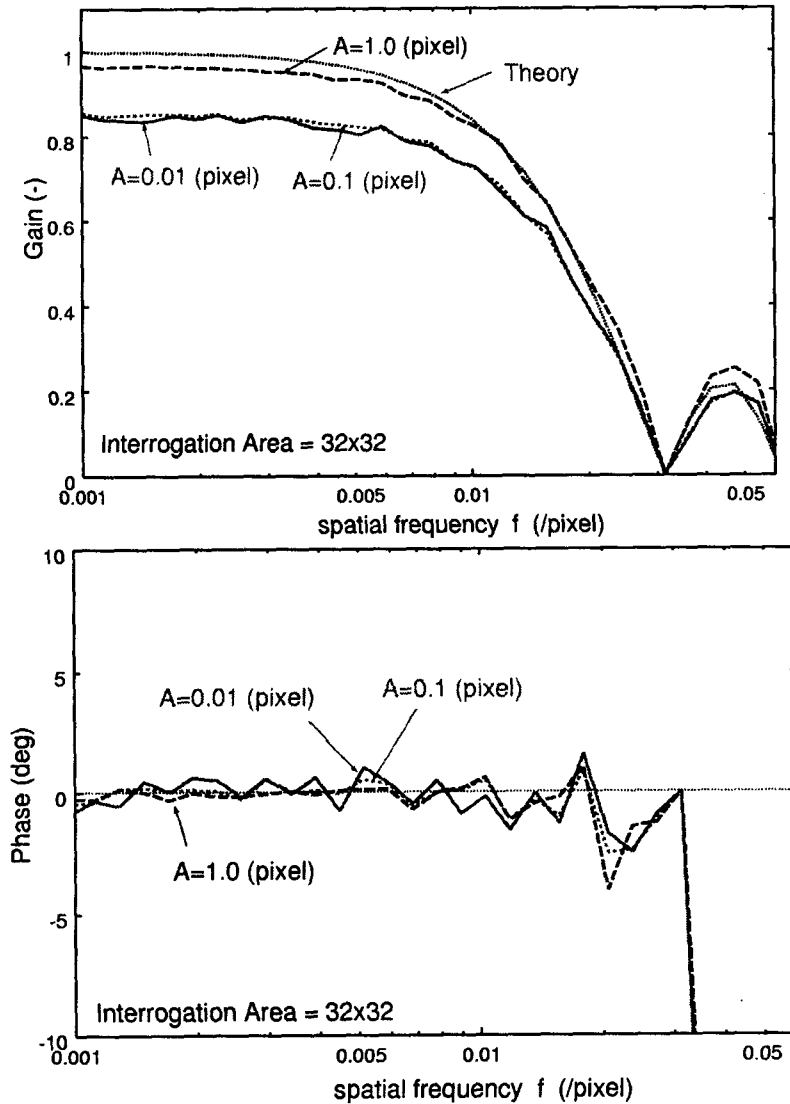
velocity field correctly under larger amplitude case ( $A > 0.1$  pixel). Since the interrogation area is 32 pixel, the frequency larger than  $1/32$  ( $=0.03$ ) could not be detected. For practical use, the  $0.007 \text{ pixel}^{-1}$  is the maximum frequency. This means that the detectable fluctuation amplitude is larger than  $120 \text{ pixel}$ . In the PIV results, much smaller fluctuation data were reported. However, these data do have relatively larger gain loss. To detect high

spatial frequency data, much smaller interrogation area should be needed. The relationship between the theoretical gain and interrogation area should be taken into account for the measurement of PIV.

For the FFT, the gain losses (about 15%) were observed in the smaller amplitude ( $A < 0.1$  pixel). In the larger case ( $A = 1.0$  pixel), the gain almost agreed with the theoretical one. The estimated amplitude might be smaller than the real one under the smaller amplitude cases. This gain loss may relate to the so called peak locking phenomena. However, they show very good phase responses even in the smaller amplitude cases, i.e., almost in the range of  $\pm 2$  degree. No phase delay was observed in the FFT analysis.

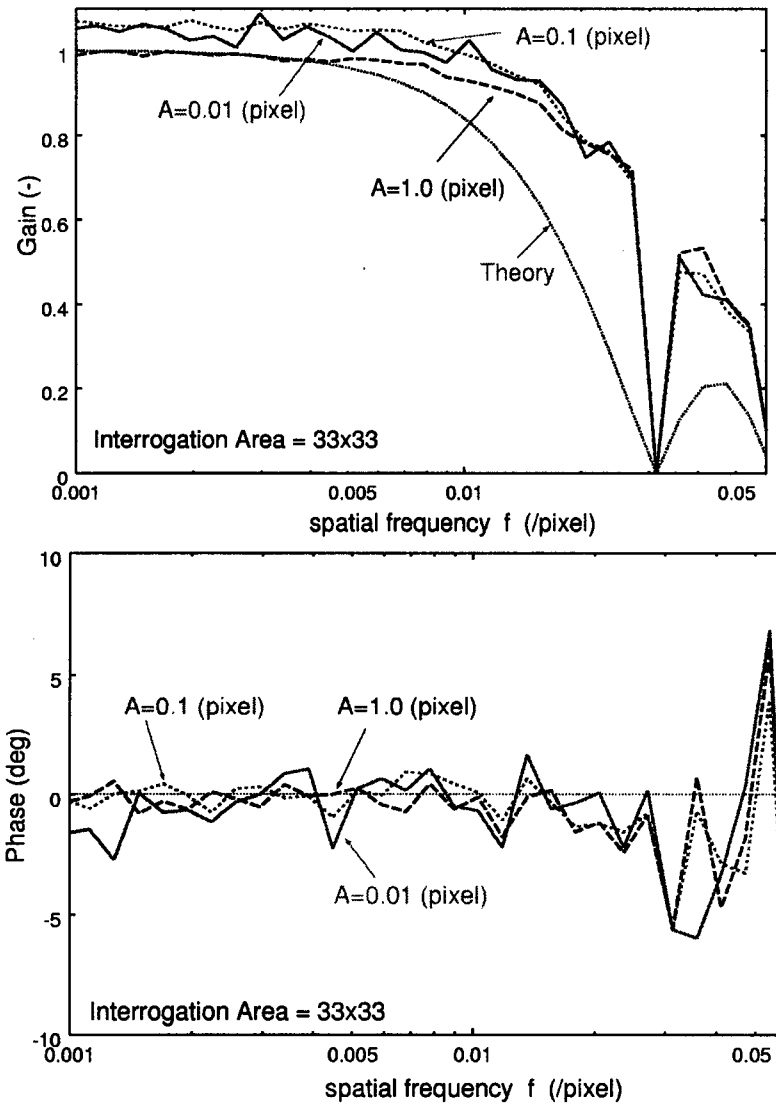
For the Gradient method, the over responses (about 8%) were observed under the smaller amplitude ( $A < 0.1$  pixel). The phase distributed in the range of  $\pm 3$  degree, showing the good reconstruction.

All of the three techniques could reconstruct the fluctuation under the larger amplitude cases. Any technique



(b) FFT cross-correlation  
 Fig. 4 Bode diagram for 32x32 interrogation area

can be applicable with larger amplitude and smaller frequency fluctuation. When the amplitude is smaller ( $A < 0.1$ ), DCC could not reconstruct the fluctuation. FFT and Gradient could reconstruct the fluctuation even in the smaller amplitude, however, the gain responses showed the under and over estimation, respectively. The reconstruction of the smaller amplitude fluctuation should be more carefully evaluated. In these three techniques, the Gradient method was superior for the estimation of the sub-pixel fluctuations.



(c) Gradient method with iteration  
 Fig. 4 Bode diagram for 32x32 interrogation area

#### 4. Small interrogation area (4x4)

In the recursive or iterative PIV technique, sometimes very small interrogation area might be used, e.g., 4x4. Also, the smaller the interrogation area, the higher spatial frequency according to Eq.(4). Therefore, to improve the PIV results, the velocity data for the smaller interrogation area should be measured high accurately. The frequency responses on the size of interrogation area were evaluated in the cases of 4x4, 8x8, 16x16. The results of 4x4 interrogation area are shown in Fig. 5.

For the DCC, the gain curve was fluctuated in the range of 0.8 to 1.2, even in the larger amplitude case. The phase also shows the larger fluctuation (upto 20 degree). Because of the smaller interrogation area, the Gaussian

peak fit technique could not be applicable. FFT was also out of applicable range. Only 16 pixels contributed the cross-correlation calculation.

However, the Gradient technique can reconstruct the flow field even in such a small interrogation area. The gain distributed in the range of 10%. The phase also shows very good responses. In the Gradient technique, the displacement was calculated in every pixel, then it was estimated in the interrogation area using the least square technique. Therefore, the information of the whole images was directly used. The amount of the contributed information for sub-pixel estimation was larger than that of FFT/DCC.

This is the reason why the gradient technique is the best technique in the sub-pixel evaluation.

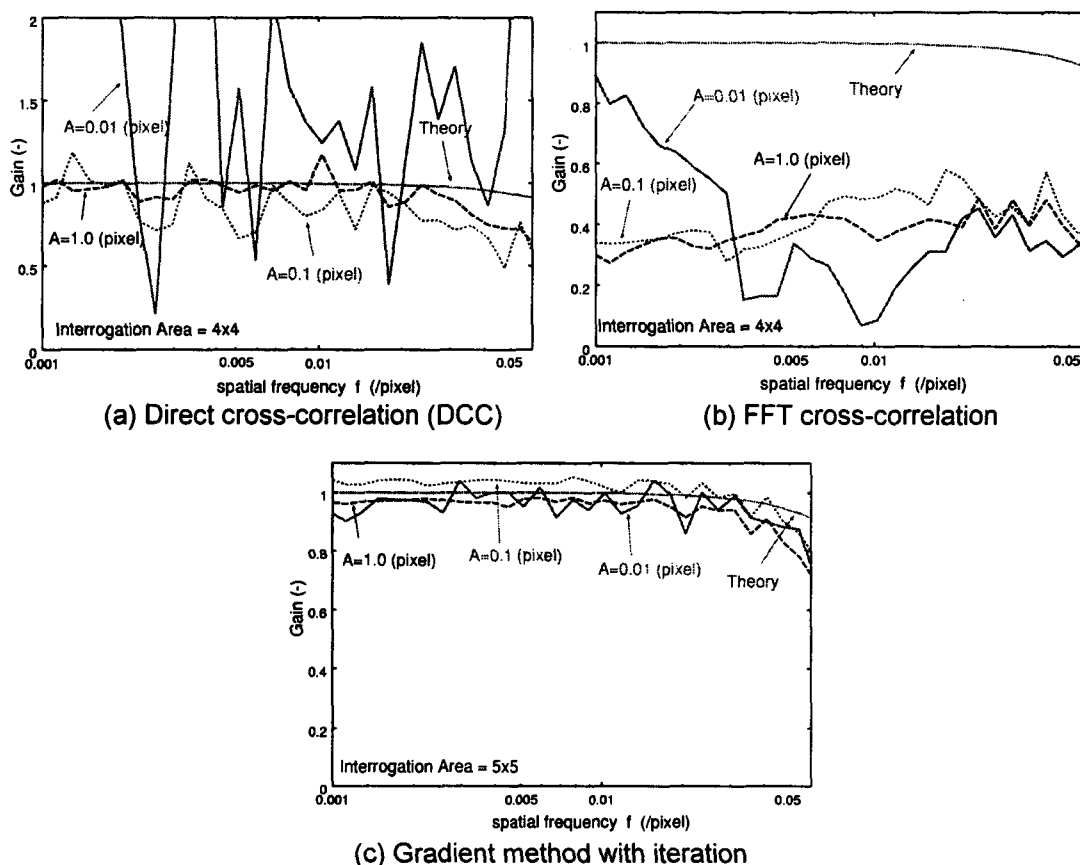


Fig. 5 Frequency response for the smaller interrogation (4x4)

## 5. Amplitude Responses

To clarify the amplitude effects, the gain response curve was re-plotted as shown in Fig. 6. The x-axis denotes the amplitude. It is clearly seen that the responses by the FFT, DCC and Gradient were good under the relatively larger amplitude cases ( $A > 0.5$  pixel). When the amplitude was less than 0.5 pixel, the gain decreases to be about 85% in FFT. It increases to be about 108% in Gradient. There exist rapid recovery about 0.5 pixel displacement. The response in DCC is almost unity.

In the small interrogation area cases (Fig.7), FFT and DCC show the very bad responses. On the other hand, the Gradient shows very good responses for all amplitude cases. The Gradient technique could be confirmed to give the very good sub-pixel estimation, especially for the small interrogation area.

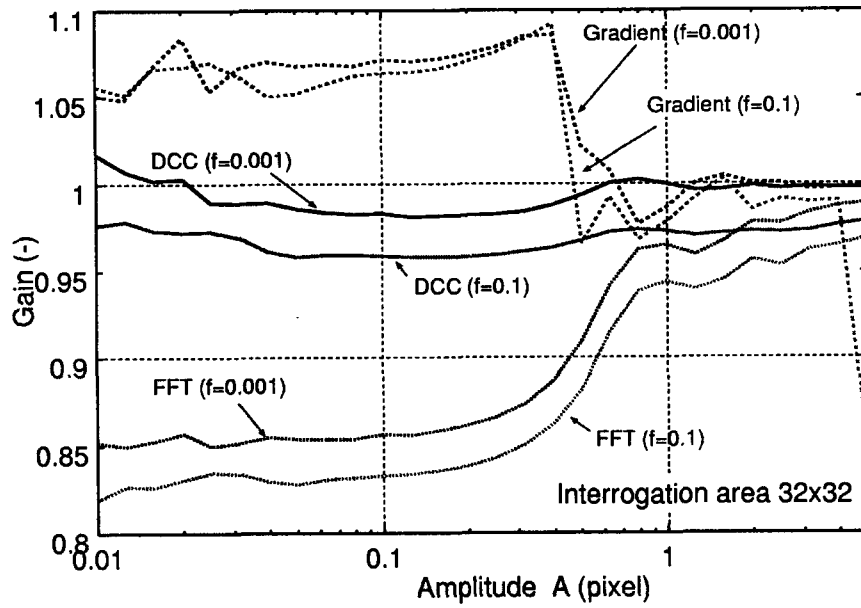


Fig.6 Gain response with amplitude for larger interrogation area (32x32)

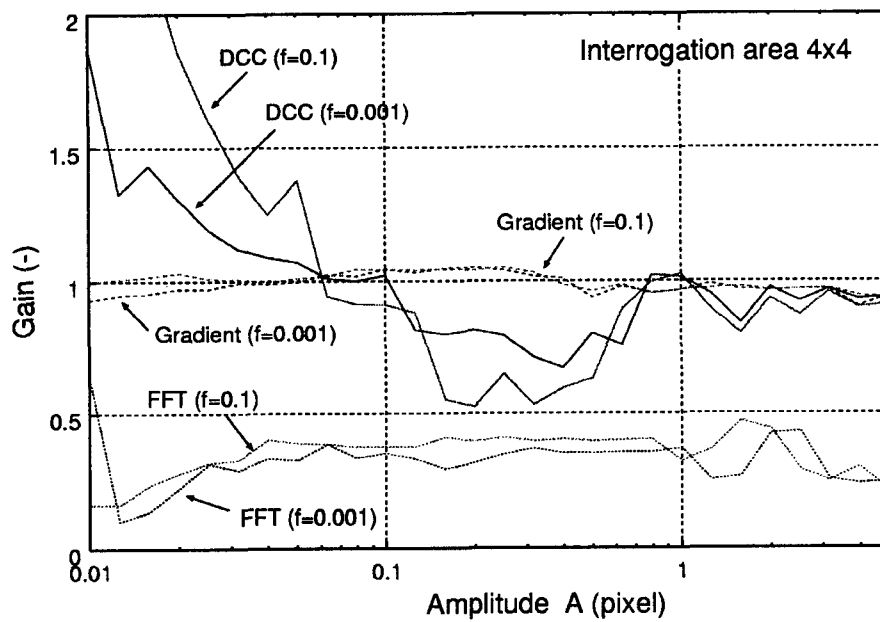


Fig.7 Gain response with amplitude for larger interrogation area (4x4)



## 6. Conclusion

The frequency response by the FFT based cross-correlation gives very good results, however, the gain loss do exist for the small displacement, (less than 0.5 pixel). While, a few gain loss is observed in the Direct Cross-correlation, however, the sub-pixel accuracy was limited to be about 0.1 pixel, i.e., it could not detect the small displacement. The Gradient technique shows very good results even in the small amplitude case. In the small interrogation area, only the Gradient technique can be applicable to estimate the sub-pixel accuracy.

For the sub-pixel analysis, the Gradient technique should be applied, especially under the condition of the small interrogation area and the smaller displacement..

## *References*

- Hart D.P., "PIV error correction", *Experiments in Fluids* 29 (2000) 13.
- Keane R, D and Adrian R.J, "Optimization of particle image velocimeters," *Meas Sci Technol*, 2 (1990), 1202
- Lecordier, B., Lecordier, J.C., Trinite, M., "Iterative sub-pixel algorithm for the cross-correlation PIV measurements," *Proc. PIV-99*, (1999), 37.
- Okamoto, K., Nishio, S., Saga, T., Kobayashi, T., "Standard images for particle-image velocimetry," *Meas Sci Technol*, 11, (2000), 685.
- Raffel, M., Willert, C., Kompenhans, J., "Particle Image Velocimetry," Springer-verlag, (1999).
- Sugii, Y., Nishio, S., Okuno Y., Okamoto, K., "A highly accurate iterative PIV technique using a gradient method," *Meas Sci Technol*, 11, (2000) 1666
- Westerweel J, Dabiri D, Gharib M, The Effect of a discrete window offset on the accuracy of cross-correlation analysis of digital PIV recordings. *Exp Fluids*, 23, (1997) 20